Capillarity

Vol. 17, No. 1, p. 1-15, 2025

Invited review

Surface acoustic wave manipulation of fluids and suspended particles in microchannels and sessile droplet: A review

Liquan Peng[1], Yan Zhou[1]*, Wei Guan[1], Fangzhou Zhao[2]

[1]*Department of Astronautics and Mechanics, Harbin Institute of Technology, Harbin 150001, P. R. China*

[2]*State Key Laboratory of Petroleum Resources and Engineering, China University of Petroleum, Beijing 102249, P. R. China*

Keywords:
Acoustofluidics
interdigitated transducers
microfluidics
surface acoustic waves
particle manipulation

Cited as:
Peng, L., Zhou, Y., Guan, W., Zhao, F. Surface acoustic wave manipulation of fluids and suspended particles in microchannels and sessile droplet: A review. Capillarity, 2025, 17(1): 1-15.
https://doi.org/10.46690/capi.2025.10.01

Abstract:
Acoustofluidic technology enables the precise motion control of microfluids and their suspended matter through microscale flow channels or acoustic streaming mechanisms, featuring multi-functionality, high throughput, dynamic controllability, fast response, high precision, and low energy consumption. In recent years, numerous literatures have reviewed the development of acoustofluidic technology, discussing the acoustic manipulation modes of particles in microfluids and their applications. However, research on the surface acoustic wave-based acoustic manipulation of particles and fluids in different microfluids remains scarce. This paper aims to provide a comprehensive review of this topic, delving into the fundamental principles of surface acoustic wave-based acoustofluidic technology and discussing the latest advancements in this field. First, the basic theory of acoustofluidic technology is introduced along with the forces involved in manipulating particles and fluids, then the advantages and disadvantages of different types of surface acoustic wave devices are reviewed. Microfluids are categorized into two main types: Fluids within microchannels and droplets on open surfaces. The surface acoustic wave-based acoustic manipulation methods for their internal fluids and suspended particles are discussed separately. Subsequently, the advantages and limitations of surface acoustic wave-based platforms in the acoustic manipulation of fluids and particles are analyzed. The work concludes with a summary of the challenges faced by acoustic streaming in the field of fluid and particle manipulation, followed by prospects for the future development of acoustofluidic technology.

1. Introduction

The field of microfluidics has emerged in response to the demand for intelligence, integration and miniaturization in modern technology (Hossein and Angeli, 2023). It enables the precise control of microscale fluids and suspended particles (e.g., cells) via microchannels or flow mechanisms, offering multifunctionality, high throughput, dynamic control, rapid response, high precision, and low energy consumption (Qi et al., 2023). As a cross-disciplinary platform, microfluidics has found broad applications in the areas of optics (Li et al., 2015; Xia et al., 2019), biomedicine (Li et al., 2017; Poudineh et al., 2017; Zhang et al., 2020b), materials physics (Huang et al., 2005; Mitragotri et al., 2015; Chen et al., 2019; Koo et al., 2023), chemistry (Sun et al., 2014; Astruc, 2020), energy (Wang et al., 2014; Kuljabekov et al., 2023), and electrical engineering (Choi et al., 2016; Zhao et al., 2021b; Jo et al., 2022). In biomedicine, microfluidics supports a range of applications: Lipid nanoparticles for drug delivery

Yandy Scientific Press

*Corresponding author.
E-mail address: Liquan.P@hotmail.com (L. Peng); zhouyan19950806@gmail.com (Y. Zhou); guanw@hit.edu.cn (W. Guan); zhaofzzz@163.com (F. Zhao).

Received June 12, 2025; revised July 7, 2025; accepted July 22, 2025; available online July 27, 2025.

(Xu et al., 2022), antibody-protein conjugates for targeted therapy (Mullard, 2021), and Deoxyribonucleic Acid (DNA) molecules for constructing complex nanostructures (Ramezani and Dietz, 2020). For instance, the efficient enrichment, screening and isolation of cells are essential for detecting specific targets in blood samples, making high-performance cell sorting critical for disease diagnosis and treatment. In addition, the pores of human skin, which is regarded as porous media, are important channels for drug delivery in vitro, and the transport mechanism within these channels has also been widely studied (Zhou et al., 2023, 2024; Cai et al., 2024). Over the past decade, microfluidics has become a powerful tool for improving sorting efficiency. According to the energy source, microfluidic technologies are classified into passive and active systems. Passive microfluidics relies on laminar flow-driven molecular diffusion, often requiring complex channel designs tailored to specific applications. In contrast, active microfluidics introduces external fields to simplify the device architecture while achieving dynamic control. Currently, active microfluidics integrates electric (Dürr et al., 2003; Deivasigamani et al., 2023; Lomeli-Martin et al., 2023), magnetic (Jang and Lee, 2000; Lee et al., 2001), optical (Wu, 2011; Zhou et al., 2022), and acoustic fields (Doinikov et al., 2018; Yang et al., 2022a), providing tunable and high-throughput alternatives to passive methods.

The advent of active microfluidics has allowed the reduction of particle and cell damage during multi-step, contact-based operations, effectively addressing the limitations of conventional methods in processing trace or rare samples (Wu et al., 2017; Song et al, 2023). Among the active techniques, acoustic tweezers stand out for their non-contact nature, label-free operation, broad applicability and excellent biocompatibility, making them highly suitable for microfluidic applications (Li et al., 2024). With recent advancements in microelectromechanical systems and the maturation of high-precision transducer fabrication, acoustofluidics has progressed significantly, leveraging high-frequency Body Acoustic Wave (BAW, 2-10 GHz) and Surface Acoustic Wave (SAW, 10 MHz-1 GHz). It currently serves as a powerful platform for the manipulation and analysis of complex particulate samples (Zhao et al., 2021a; Yang et al., 2022b).

In acoustofluidics, fluid and suspended particle motion are governed by both acoustic and hydrodynamic forces. Both BAW and SAW require a piezoelectric substrate for wave propagation (Fan et al., 2022; Liu et al., 2023b). BAW propagates through the substrate thickness, whereas SAW is confined to its surface. Compared to BAW, SAW exhibits lower energy loss, allowing equivalent control with reduced power consumption. Moreover, SAW enables the precise manipulation of submicron and nanoscale particles: By tuning their frequency and amplitude, the acoustic forces exerted on fluids and particles can be modulated, enabling accurate control and selective manipulation within microfluidic environments (Zhang et al., 2020a).

Acoustofluidic technology for fluid and particle manipulation has advanced rapidly, with manipulable particle sizes shrinking from the micrometer scale to below 100 nm within a few decades (Wiklund et al., 2012; Zhang et al., 2021). Particle

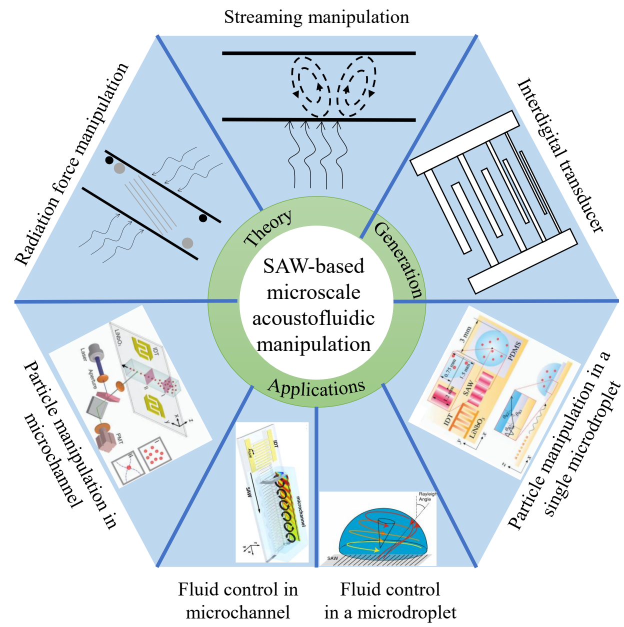

Fig. 1. Overview of acoustofluidic manipulation for particles and fluid.

manipulation efficiency is highly size-dependent. For micron- and submicron-sized particles, motion is primarily governed by acoustic radiation force, enabling effective capture, separation and enrichment. In contrast, for nanoparticles (10-100 nm) commonly used in biomedical applications such as targeted drug delivery, acoustic streaming is becoming the dominant mechanism, while its effectiveness is limited by Brownian motion. Consequently, higher acoustic intensity or alternative excitation strategies are required to maintain control over such small particles (Gu et al., 2021). Recent studies have demonstrated that tilted, high-frequency SAW with increased acoustic intensity significantly enhances the precision and efficiency of nanoscale particle manipulation (Lee et al., 2024; Peng et al., 2024). While these advances have improved sorting, trapping and concentration with lower energy consumption and higher spatial resolution, SAW-based techniques still face challenges in complex fluidic environments. In practice, achieving the accurate manipulation of diverse particle types with a single-frequency, a single-intensity SAW device remains insufficient.

Recent reviews have summarized the development of acoustofluidics and the acoustic manipulation modes in microfluidic systems (Hossein and Angeli, 2023; Qi et al., 2023; Amorim et al., 2025; Hsu, 2025). However, comprehensive analyses focusing specifically on the SAW-based manipulation of particles and fluids across different microfluidic environments remain limited. This gap is particularly evident in biomedical applications, where the precise and efficient separation or screening of cells, viruses and secretions is often required in sessile droplets or microchannels. To address this challenge, the present review offers a systematic overview of SAW-based acoustofluidic manipulation techniques, covering the fundamental principles, device configurations, and recent technological advances. First, the theoretical basis of acoustic streaming is introduced and the forces involved in fluid and particle manipulation are discussed. Then, various SAW-generating devices are examined, analyzing their advantages and limitations. Microfluidic systems are categorized into two types: Enclosed microchannels and open-surface droplets, as shown in Fig. 1. SAW-based manipulation strategies for fluids and suspended particles in each system are discussed separately, along with a critical evaluation of their performance, benefits and constraints. The review concludes by outlining the current challenges and forecasting the future directions for SAW-based acoustofluidics in particle and fluid manipulation.

2. Theory of SAW for microfluidics manipulation

2.1 Perturbation theory

In acoustic devices, applying an electrical signal to a piezoelectric material induces resonance in its crystal structure, generating acoustic waves. Two primary types are produced: BAW, which propagates through the bulk of the material, and SAW, which travels along its surface (Ali and Prasad, 2020). These vibrations transfer into the fluid, generating acoustic waves through perturbations in fluid density and pressure under quasi-equilibrium conditions. Since the relative change in fluid density induced by sound waves is typically less than 1%, acoustic waves are treated as first-order effects in fluids. However, due to the fluid's inherent nonlinearity, the convective derivative in the momentum equation introduces second-order effects, resulting in a steady fluid flow known as acoustic streaming. This phenomenon is a secondary effect that forms the basis of acoustofluidics (Kaushik, 2022). Perturbation theory, applicable to low-velocity regimes where fluid speed is much lower than the speed of sound, is commonly used to model these effects (Orosco and Friend, 2022). In biomedical applications, fluids such as water or saline are typically used, with flow velocities in the micron range-well below the speed of sound in water (1,500 m/s)–thus satisfying the conditions for perturbation analysis. Under this framework, disturbances in pressure (p), density (ρ) and velocity (v) are expressed as series expansions, with first-order and second-order terms denoted by subscripts 1 and 2, respectively (Wei et al., 2024):

$$\begin{cases} p = p_0 + p_1 + p_2 \\ \rho = \rho_0 + \rho_1 + \rho_2 \\ \boldsymbol{v} = \boldsymbol{v}_0 + \boldsymbol{v}_1 + \boldsymbol{v}_2 \end{cases} \tag{1}$$

where p_0, ρ_0 and $\boldsymbol{v}_0$ represent hydrostatic pressure, density and velocity vectors, respectively. This formulation highlights the primary effect of sound waves in fluids: They propagate as pressure waves that cyclically compress and expand the medium, enabling acoustic energy transmission. However, fluid viscosity leads to a gradual attenuation of wave intensity. By substituting the first-order solution into the second-order equation and applying time averaging, the acoustic streaming field can be derived, comprising both oscillatory and steady-state components. The time-averaged second-order pressure p_2 acts on the suspended particles, generating acoustic radiation forces. Overall, acoustofluidic effects represent the combined impact of acoustic energy and momentum transfer on nanoparticles in fluid. This interaction results in both acoustic radiation force and streaming-induced drag force, driven by the stabilized acoustic streaming flow.

2.2 Acoustic radiation force for manipulation

Particles suspended in an acoustic field are subject to time-averaged forces arising from wave scattering, known as acoustic radiation forces, which are classified into primary and secondary types. Primary acoustic radiation forces result from the direct interaction between sound waves and submicron to nanoscale particles in a fluid, while secondary forces originate from inter-particle interactions mediated by the scattered waves within the medium (Wu et al., 2013). In a non-viscous fluid under ultrasound, if the radius a of suspended compressible particles is much smaller than the acoustic wavelength λ_f (i.e., $a \ll \lambda_f$), they act as weak scatterers. The resulting acoustic radiation force can be derived using the first-order scattering theory. Denoting the velocity of the incident wave as $\boldsymbol{v}_{in}$ and the scattered wave as $\boldsymbol{v}_{sc}$, the first-order acoustic velocity field can be expressed as:

$$\boldsymbol{v}_1 = \boldsymbol{v}_{in} + \boldsymbol{v}_{sc} \tag{2}$$

For a given first-order incident field $\boldsymbol{v}_{in}$, once the scattered field $\boldsymbol{v}_{sc}$ has been determined, the acoustic radiation force $\boldsymbol{F}^{rad}$ on the particle can be calculated as a time-averaged second-order force on a fixed surface $\partial\Omega$ in a nonviscous fluid. The conservation of momentum and zero volume force ensure that any fixed surface can be chosen; for an inviscid fluid, $\boldsymbol{F}^{rad}$ equals the sum of the time-averaged second-order pressure and momentum flux, with its expression given as (Zhang and Chen, 2021):

$$\boldsymbol{F}^{rad} = -\int_{\partial\Omega} \mathrm{d}a \left\{ \left[\frac{\kappa_0}{2}\langle p_1^2 \rangle - \frac{\rho_0}{2}\langle \boldsymbol{v}_1^2 \rangle \right] \boldsymbol{n} + \rho_0 \langle (\boldsymbol{n}\cdot\boldsymbol{v}_1)\boldsymbol{v}_1 \rangle \right\} \tag{3}$$

where κ_0 represents the particle compression coefficient and $\boldsymbol{n}$ is the unit normal vector on the particle surface pointing toward the fluid.

2.3 Acoustic streaming force for manipulation

Acoustic streaming, a nonlinear flow phenomenon induced by sound wave propagation in a fluid medium, manifests as vortices or jets characterized by specific velocities, length scales and flow geometries. The hydrodynamic pattern of acoustic streaming is influenced by various features of the acoustic field, such as boundary conditions and acoustic attenuation coefficients.

In acoustic streaming applications, classical acoustic streaming terminology is often used, such as Eckart acoustic streaming, Rayleigh acoustic streaming, Schlichting acoustic streaming, and Oscillating microstreaming (Lighthill, 1978). Eckart acoustic streaming is formed by the dissipation of acoustic energy into a fluid. As sound waves propagate through a fluid, a portion of the sound energy is absorbed by the fluid at a rate proportional to the square of the frequency of the sound wave. Thus, the amplitude of the sound wave is weakened, causing the sound pressure amplitude to decrease as it moves away from the source. The loss of acoustic energy causes momentum flow, the formation of fluid jets inside the acoustic beam in the direction of sound propagation, and the generation of vortices in the microfluidic cavity or part of the cavity. To produce significant Eckart sound flow, the dimensions of the chamber that forms the propagation length of the sound wave must be comparable in length to or greater than the acoustic attenuation length. If the dimensions of the fluid are smaller than the acoustic attenuation length, such streaming may not occur. This phenomenon is driven by a volumetric force, engendered by the sound wave, which impels the fluid in a designated direction. This force is the cornerstone of the acoustofluidic effect and is intrinsically linked to the vibrational velocity field of the sound wave. When determining the volumetric force, it is imperative to ascertain the acceleration response of the fluid to the acoustic stimulus. The volumetric force can be expressed as (Friend and Yeo, 2011):

$$\boldsymbol{F}_{dc} = -\langle(\boldsymbol{v}_1 \cdot \nabla)\boldsymbol{v}_1\rangle + \frac{1}{\rho_{dc}^2}\left[\langle\rho_1\nabla\rho_1\rangle - \mu\langle\rho_1\nabla^2\boldsymbol{v}_1\rangle - \left(\eta+\frac{\mu}{3}\right)\langle\rho_1\nabla\nabla\cdot\boldsymbol{v}_1\rangle\right] \tag{4}$$

where the subscript dc represents the steady-state value of the associated second-order component, and η and μ denote the volume viscosity and fluid viscosity, respectively. When the acoustic streaming described above acts on a particle, the velocity of the fluid at the surface of the particle must be equal to the velocity of the particle, which is the no-slip boundary condition. Suppose that the external force moves a spherical particle p of radius a with velocity $\boldsymbol{v}$, while the fluid itself leaves the particle with velocity $\boldsymbol{v}$. This implies that there is a relative velocity difference between the particle and the fluid. Due to the viscous effect of the fluid, as the particle moves, it is subjected to a drag force, called Stokes drag force "$\boldsymbol{F}$", which can be expressed as:

$$\boldsymbol{F}_{dc} = \int_{\Omega_p} \mathrm{d}a\left(-p\boldsymbol{n} + \boldsymbol{\sigma}'\cdot\boldsymbol{n}\right) = 6\pi\eta a\left(\boldsymbol{v}-\boldsymbol{v}_p\right) \tag{5}$$

Rayleigh acoustic streaming (Nyborg, 2024) refers to the acoustic streaming phenomenon occurring within the fluid, aligned parallel to the propagation direction of acoustic waves. This streaming is marked by substantial energy dissipation and pronounced velocity gradients within the boundary layer. Usually occurring in a vortex mode with vortex dimensions of the same order of magnitude as the wavelength, it describes the mechanism by which the fluid flow matches the flow at the edge of the boundary layer. The thickness of the viscous boundary layer (δ_V) is based on the viscosity (μ), density (ρ_f) and acoustic frequency (ω) of the fluid:

$$\delta_V = \sqrt{\frac{2\mu}{\omega\rho_f}} \tag{6}$$

Schlichting acoustic streaming is the streaming of sound within a viscous, incompressible boundary layer toward a sound source due to viscous attenuation. Because the viscous boundary layer is typically much smaller than the wavelength of the sound wave, this streaming type is the finest of the three. The dominance of one form of flow over another in a fluid field, as well as the possibility of all three forms of flow, can lead to highly complex physical phenomena, and the determination of the presence or dominance of these forms of acoustic streaming in a fluid usually depends on the size of the fluid system.

Oscillating microstreaming is an acoustic flow effect resulting from the viscous attenuation of acoustic waves near the fluid boundary of a stable oscillating object. Depending on the acoustically oscillating object, oscillating microstreaming can be divided into two main categories: Oscillations with sharp edges (Akthakul et al., 2005) and those with microbubbles (Zhao et al., 2011). When alternating current or radiofrequency excitation is applied to an electrode on a piezoelectric material, a BAW propagates into the bulk medium in a direction perpendicular to the material surface. The sharp edges oscillate with the acoustic wave, generating a pair of counter-rotating acousto-hydrodynamic vortices at the tip position. Bubble microflows (Liu et al., 2002) are caused by steady oscillations of microbubbles in the acoustic field. In this case, the viscous-induced attenuation of the acoustic waves in the boundary layer surrounding the microbubbles eventually leads to a local amplification of the first-order velocity. Consequently, flow velocities will result that significantly exceed those around incompressible particles. The efficacy of microbubbles within the acoustic field is intrinsically linked to their resonance properties, and the resonance frequencies can be expressed as:

$$2\pi rf = \sqrt{\frac{3\gamma P_0}{\rho}} \tag{7}$$

where r represents the radius of the microbubble, f represents the resonant frequency, γ denotes the ratio of specific heats of the gas, P_0 denotes the hydrostatic pressure, and ρ is the density of the liquid medium.

3. Principles of preparation and design of SAW devices

Interdigital Transducer (IDT) is a fundamental component of SAW devices, patterned on the surface of a piezoelectric substrate. It comprises at least one pair of interleaved metal electrodes arranged orthogonally, with converging electrodes at both ends to facilitate SAW excitation and detection, enabling bidirectional conversion between electrical and acoustic signals. The structural configuration of IDT directly determines the bandwidth and propagation direction of the generated SAW.

The wavelength of the SAW, λ_s, is defined by the width m of the metal fork-finger electrodes and the fork-finger pair spacing n. The classical design scheme is $\lambda_s/4 = n/2 = m$, which excites the strongest SAW with the IDT called a uniform transducer, as shown in Fig. 2(a). The SAW velocity c_s depends on the material properties of the piezoelectric substrate, the propagation direction, and the thickness of the IDT. Therefore, the center frequency of a SAW device is determined by a combination of piezoelectric substrate properties, propagation direction, and IDT design. The structure of the IDT determines the bandwidth and direction of the generated SAW, and the acoustic properties of the SAW can be changed

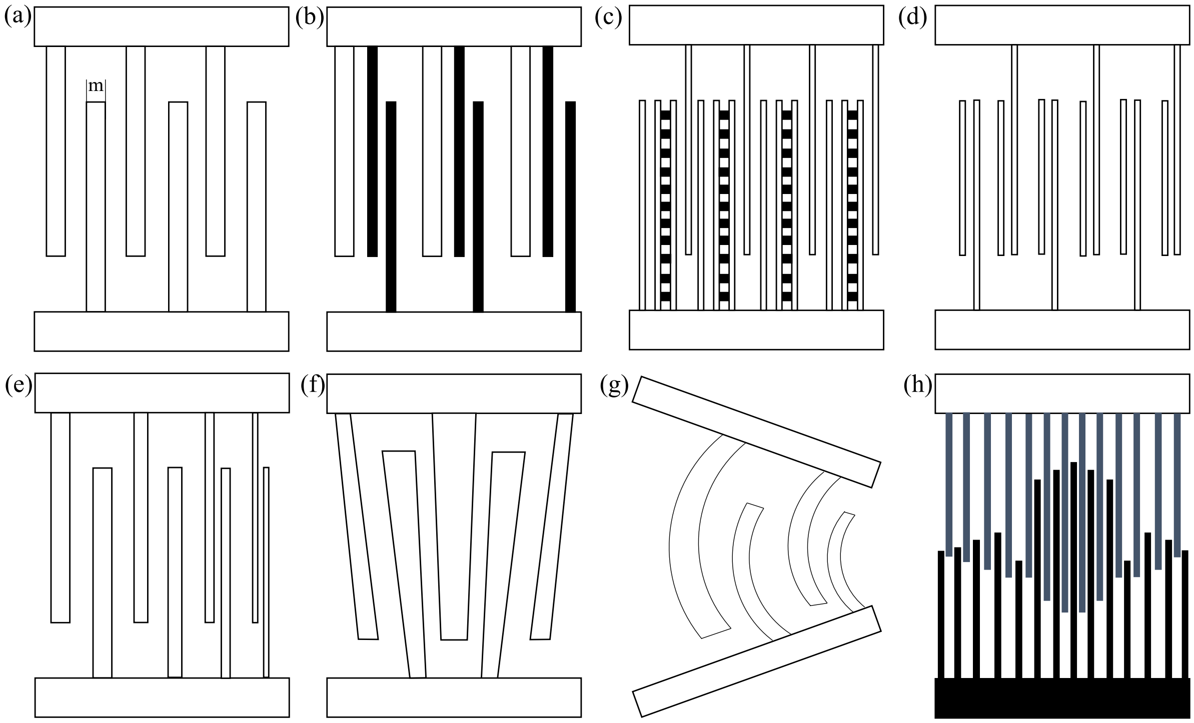

Fig. 2. Structure diagram of interdigital transducer. (a) Straight uniform IDT (Potter et al., 2016), (b) single-phase unidirectional IDT (Nakagomi et al., 2003), (c) distributed acoustic reflection IDT (Shui et al., 2002), (d) floating electrode unidirectional IDT (Kondoh et al., 2008), (e) dispersed delay line IDT (Ding et al., 2012a), (f) conical IDT (Ding et al., 2012b); (g) focused IDT (Zhou et al., 2019) and (h) variable trace IDT (Bausk et al., 2003).

by varying the number, spacing and aperture diameter of the fork finger electrodes.

SAW devices in acoustic fluidics typically operate in the range of 1 MHz to 1 GHz. Using 128°Y-X $LiNbO_3$ as the substrate yields acoustic wavelengths (λ_s) from 4-200 μm, corresponding to IDT feature sizes of 1-50 μm, which are fabricated via UV lithography. Fig. 2 presents various IDT structures for microfluidic actuation and sensing, which are listed as follows:

(a) Straight uniform IDT (Potter et al., 2016): A simple and widely used design that generates bidirectional SAWs with equal energy.
(b) Single-phase unidirectional IDT (Nakagomi et al., 2003): It incorporates a reflector grid to suppress regenerative waves, enabling unidirectional SAW transmission and reducing insertion loss. However, overall SAW energy is diminished, limiting excitation efficiency.
(c) Distributed acoustic reflection IDT (Shui et al., 2002): It comprises periodic cells (length = λ_s), with two electrodes of $\lambda_s/8$ width, one of $3\lambda_s/8$ width and with a spacing of $\lambda_s/8$. This design eliminates net reflection and transmission and allows adjustable reflectivity via electrode segmentation.
(d) Floating electrode unidirectional IDT (Kondoh et al., 2008): It features at least one electrically isolated electrode per unit cell. By configuring open or shorted terminals, it enables the directional control of SAW propagation.
(e) Dispersed delay line IDT (Ding et al., 2012a): It uses a gradient in electrode width and spacing to generate a broadband SAW spectrum with tunable frequency response.
(f) Conical IDT (Ding et al., 2012b): It varies electrode periodicity along the aperture length to achieve frequency-dependent SAW direction control, enabling wide bandwidth and dynamic droplet actuation.
(g) Focused IDT (Zhou et al., 2019): It concentrates acoustic energy into a localized area, enhancing pumping, mixing and sensing performance.
(h) Variable trace IDT (Bausk et al., 2003): It adjusts fork-finger edge profiles to achieve target waveforms and frequency responses. The extended resonance path increases attenuation modes and reduces transverse spurious signals.

4. SAW-based microfluidic devices for manipulation

The previous section introduced SAW generation devices and the physical effects induced when SAWs interact with fluids, which are fundamental to all acoustofluidic systems. Depending on the wave excitation mode, SAW-based microfluidic manipulation techniques are generally classified into Traveling SAW (TSAW) and Standing SAW (SSAW) approaches. SAWs have been widely employed for one- dimensional and two-dimensional particle patterning, with successful applications in cell counting, spacing control and particle enrichment.

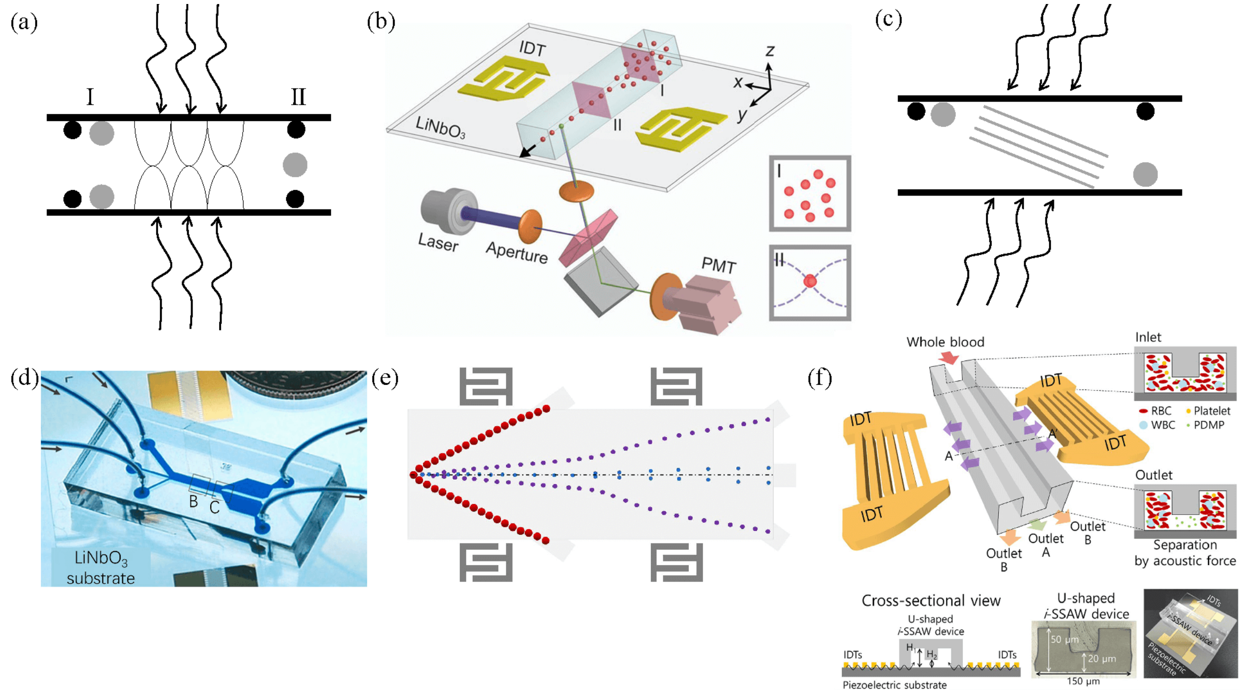

Fig. 3. Aggregation and sorting of biological particles achieved by SSAW excitation of microfluidics. (a) Schematic diagram of the action of single-node SSAW on particles, (b) cell-centered aggregation equipment (Chen et al., 2014), (c) schematic diagram of the action of single-node TSSAW on particles, (d) tilted standing surface acoustic wave particle separation equipment (Ding et al., 2014), (e) two-step SSAW-based model for particle separation (Chen et al., 2022) and (f) recessed standing surface acoustic wave device with U-shaped microchannels (Lim et al., 2025).

4.1 SSAW manipulation of microfluids

SSAW excitation in microfluidics is primarily applied for particle manipulation, with the manipulation pattern determined by the number of acoustic pressure nodes within the microchannel. A classical configuration involves a single node, as shown in Fig. 3(a), which facilitates particle aggregation at the fluid center. Chen et al. (2014) achieved focused cell aggregation in the absence of sheath flow using a single-node SSAW and integrated it with a laser-induced detection system for accurate cell counting. Owing to the particle size dependence of the acoustic radiation force, this method also enables size-based particle sorting. An alternative configuration employs multiple nodes, offering relaxed alignment requirements between the microchannel and the electrodes. Using this multi-node approach, Ai et al. (2013) successfully separated fluorescent particles and biological cells from mononuclear erythrocytes. Ding et al. (2014) proposed a design with multiple tilted SSAW nodes to further improve the sorting efficiency, where the IDT is tilted with respect to the microchannel, as shown in Fig. 3(d). This configuration allows particles that escape one node to be recaptured by downstream nodes, enhancing separation reliability. Although theoretical separation is possible across tilt angles from 0° to 90°, the experimental results indicate optimal performance at 10° to 15°.

Microfluidic structures incorporating multiple SSAW nodes are primarily used for capturing and arranging suspended particles, and their configurations can be modulated to enable diverse particle manipulation strategies. Recently, such systems have been applied to cell culture and the investigation of intercellular interactions. For instance, Chen et al. (2022) proposed a two-step SSAW-based design for separating particles of three different sizes, as shown in Fig. 3(e). Lim et al. (2025) developed a recessed SSAW device featuring U-shaped microchannels for isolating platelet-derived microparticles from whole blood, as shown in Fig. 3(f)). The influence of channel cross-sectional geometry on separation efficiency was evaluated using rectangular and U-shaped channels of varying heights, with blood samples at a hematocrit level of 40%.

In addition, orthogonal standing surface acoustic wave fields with similar frequencies generated using two pairs of forked finger electrodes are superimposed to form a two-dimensional standing wave field. The two-dimensional SSAW allows not only for particle dispersion but also for the manipulation of individual particles in a predetermined trajectory. Fakhfouri et al. (2023) introduced a method to complement the otherwise competing acoustic streaming and acoustic radiation effects by realizing rigid microchannels reproducibly and with high precision to reliably drive the microchannel cross-section, as shown in Fig. 4(a). The synergetic effect of both mechanisms markedly enhanced the manipulation of nanoparticles, down to 200-nm particles, even at relatively large wavelength (300 μm). Pan et al. (2024) proposed a reconfigurable particle capture strategy that integrates morphologically tunable magnetic micropillar arrays with SAW-induced acoustic streaming, as shown in Fig. 4(b). Neodymium–iron–boron powders were assembled into porous, shape-adaptable micropillars via

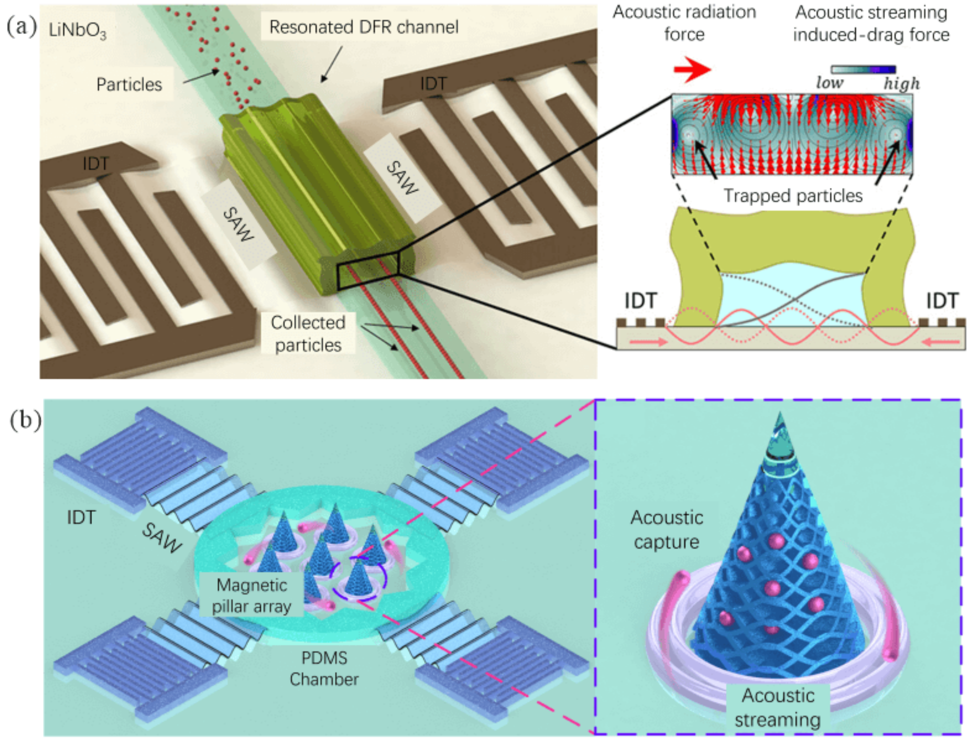

Fig. 4. Modulation of standing surface acoustic wave fields in microfluids. (a) The SAW-driven channel resonance principle utilizes laminated dry film resist fabrication, demonstrated by the enrichment of particles as small as 100 nm (Fakhfouri et al., 2023) and (b) schematic view of the proposed acoustofluidic capture and manipulation device based on reconfigurable magnetic micropillars (Pan et al., 2024).

a magnetic gradient field. The localized streaming enabled these micropillars to trap nearby particles or induce fluid perturbations for cargo transport.

4.2 TSAW manipulation of microfluids

4.2.1 Fluid control in a single microdroplet

Increasing the power of TSAW may result in droplet ejection and atomization when the radiation pressure inside the droplet is greater than the surface tension, as shown in Figs. 5(a) and 5(b), which can be initially evaluated using the Weber number *We* (Falkovich, 2011), i.e., $We = \rho_f v^2 L/\sigma$, where L denotes the microdroplet characteristic length, v denotes the fluid velocity, and σ is the fluid surface tension. This physical process is very complex and involves nonlinear effects in fluid dynamics, while quantitative theoretical studies in this area are still lacking. Currently, the phenomena of spraying and atomization of liquid droplets excited by surface traveling waves are mainly focused on via experimental applications, such as the realization of precise extraction of minute quantities of liquid from a wet paper connected to a reservoir (Qi et al., 2008; Vuong et al., 2013). Rajapaksa et al. (2014) applied this technique to a drug delivery device for shear-sensitive biomolecules.

Wixforth et al. (2004) experimentally demonstrated the acoustic streaming field mixing effect within a droplet under TSAW excitation. Shilton et al. (2014) used ultra-high frequency (1.1 GHz) SAW to generate strong acoustic streaming fields in nanoliter droplets ($\geq$ 100 μm diameter), where the attenuation length of the leakage wave within the droplet volume and at the solid-liquid interface were 50 and 20 μm, respectively, much smaller than the droplet diameter. Raghavan et al. (2010) found that when the TSAW excites a droplet asymmetrically, a unidirectional acoustic streaming rotating around a certain tilt angle is formed inside the droplet, as shown in Fig. 5(c), and its flow velocity is larger than that of the symmetrical excitation. On this basis, the team proposed asymmetric excitation of droplets by surface waves as a way to improve the internal mixing efficiency while maintaining the shape of the droplets, and they also proposed several methods to make the surface waves asymmetrically excited droplets, as shown in Fig. 5(c).

4.2.2 Particle manipulation in a single microdroplet

The acoustic streaming field generated inside the microdroplets under the excitation of TSAW not only produces a mixing effect but also achieves the aggregation or separation of suspended particles of different densities and sizes in the droplets by utilizing its tunable characteristics. As shown in Fig. 6(a), Bourquin et al. (2014) used acoustic streaming generated in a droplet under surface wave excitation to achieve the enrichment of rare cells, in order to perform rapid diagnostics on the cells. Gu et al. (2021) designed a more novel particle separation device based on droplets, which uses two tilted fork fingers to differentially separate particles of different size in two neighboring droplets. This has been successfully

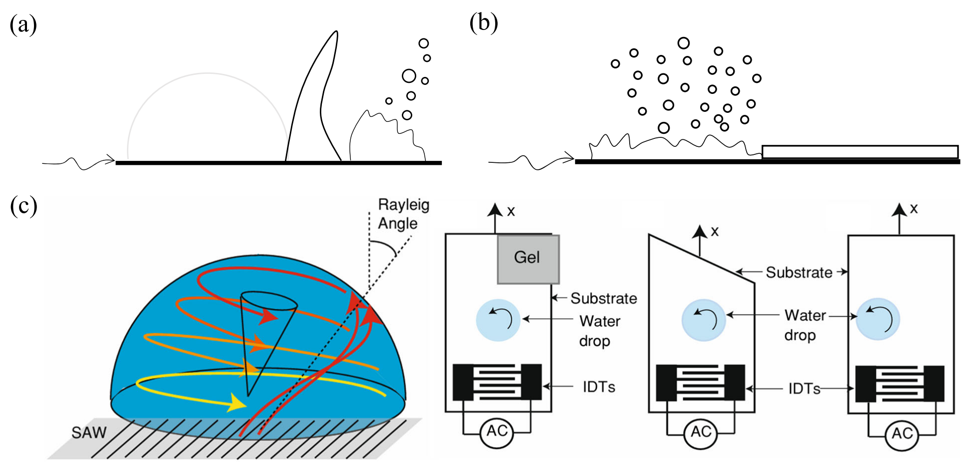

Fig. 5. Fluid motion in a single microdroplet under TASW excitation. (a) Jetting pattern of droplets, (b) atomization pattern of droplets and (c) various symmetry-breaking configurations used to generate asymmetrical SAW radiation into a drop (Raghavan et al., 2010).

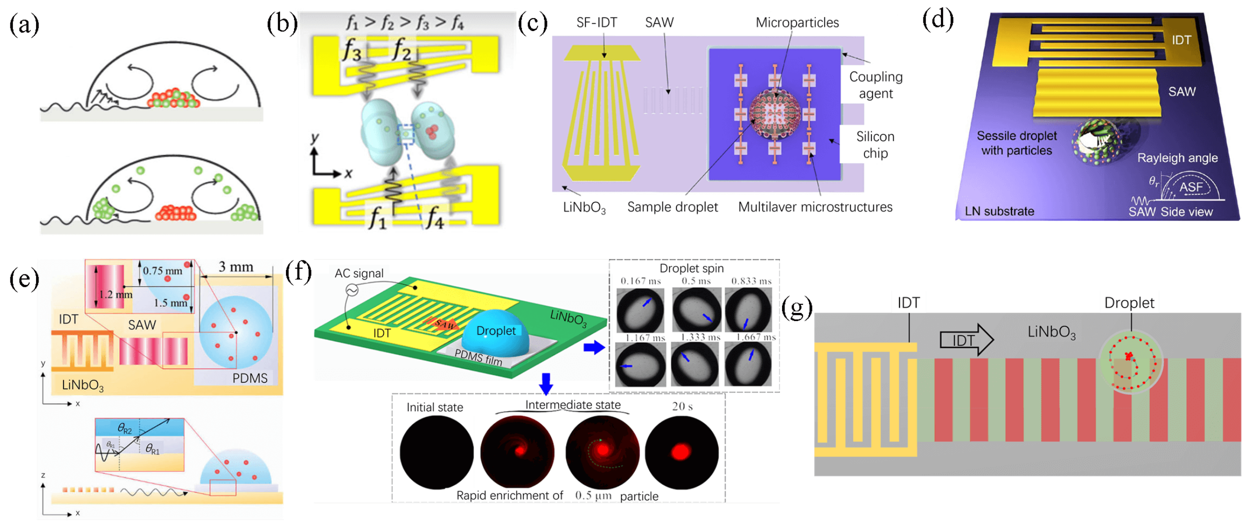

Fig. 6. Particle manipulation in microdroplets under TSAW excitation. (a) Flows induced by the TSAW (Bourquin et al., 2014), (b) schematic of the dual-droplet acoustofluidic centrifuge (Gu et al., 2021), (c) schematic of plug-and-play integrated setup (Qian et al., 2021), (d) IDT device Schematic (Destgeer et al., 2017), (e) schematic of the experimental setup (Nam et al., 2022), (f) droplet deformation and spin and the submicron particles concentration (Peng et al., 2021) and (g) schematic of diamond nanoparticle concentration (Akther et al., 2021).

applied to the separation of DNA fragments and exosomes, as shown in Fig. 6(b). Qian et al. (2021) verified the integration performance of a microdroplet-based surface wave micro-centrifugal detachable device on a membrane plate. The device uses a coupling layer to transfer the surface wave energy to the upper substrate, causing acoustic streaming and thus particle aggregation in the uppermost microdroplets, and characterizes the particles with the help of the sensing structure of the upper chip, as shown in Fig. 6(c). Destgeer et al. (2017) utilized the method of symmetrical excitation of droplets by surface waves to realize the separation of particles of different sizes by virtue of the difference in acoustic streaming velocity generated before and after the inside of the droplets. The effect of droplet contact angle on the separation effect was also considered, as shown in Fig. 6(d).

As shown in Fig. 6(e), Nam et al. (2022) investigated the effects of SAWs on cancer cell behavior within sessile droplets, initially using polystyrene particles to characterize internal dynamics. By varying the contact angle of the droplet, they assessed how droplet volume influences particle motion. As shown in Fig. 6(f), under the combined effects of acoustic streaming, droplet deformation and spinning, submicron particles follow helical trajectories and rapidly concentrate toward the droplet center. Building on this, Peng et al. (2021) achieved a spin velocity of 26,700 rpm at 28 dBm in a 1.5 µL droplet actuated by a 32.26 MHz SAW on a PDMS substrate. Similarly, Akther et al. (2021) employed SAWs to concentrate diamond nanoparticles into localized clusters within the detection field, significantly reducing measurement acquisition time due to the increased density of nitrogen-vacancy centers, as shown in Fig. 6(g). They attributed the enhanced concentration efficiency to the high density and acoustic contrast of diamond nanoparticles relative to typical cells and particles previously studied under SAW-induced recirculation flow.

4.2.3 Fluid manipulation in microchannels

The fluid in the acoustic streaming field achieves mixing through the acoustic streaming field generated by the coupling of TSAW with the fluid wrapped by the microchannels, as shown in Fig. 7(a). Destgeer et al. (2014) designed a circular fork-finger structure that yielded a unidirectionally focused surface wave field to improve mixing efficiency. In this system, the pulsed signal is used to control the switching of the surface waves, which enables the regulation of the solution concentration gradient within the microchannel, as shown in Fig. 7(b). In addition, the form of acoustic streaming field development in microchannel fluids is related to the fluid geometry. Tiller analyzed the effect of the geometry of microchannel cavity on the acoustic streaming mixing efficiency and subsequently proposed a method for selecting the optimal excitation frequency based on the microchannel geometry (Tiller et al., 2017). By changing the shape of the microchannel device to a curved surface, an acoustic streaming field can be generated in an arbitrary volume of microfluid, thus facilitating the biochemical reaction, as shown in Fig. 7(c) (Zhang et al., 2019). Meng et al. (2015) designed a device consisting of a circular fork-finger structure and circular microchannels for drug release and proposed the concept of miniature high-intensity focused ultrasound, as shown in Fig. 7(d).

Recent studies have shown that TSAW in microfluidic devices can produce periodic time-averaged acoustic fields. This is caused by diffraction effects induced by spatially constrained probes. Kolesnik et al. (2021) demonstrated the emergence of geometrically correlated acoustic vortices. They showed that the periodic application of a moving SAW can produce isotropically rotating Rayleigh flow vortices, and that the channel dimension determines the type of streaming developed. While Eckart flows were previously considered a prominent feature of traveling wave drives, Rayleigh flow vortices are also generated, as shown in Fig. 7(e). This has implications for microfluidic actuation, where traveling acoustic waves can be used for microscale mixing, separation and patterning. Li et al. (2022) investigated the temporal acoustic and flow fields of finite duration TSAW excitation. Taking the perturbation theory of slow flows as a basis, a concept of unsteady time-averaged large-scale flows was proposed, in which slow variations in flow velocity can be detected on time scales much longer than the acoustic period, as shown in Fig. 7(f). On the basis of the separation of build times, they presented a hybrid time-frequency scheme for efficient finite element analysis, which opens the way to the design of devices with additional features in the time domain.

4.2.4 Particle manipulation in microchannels

Particle manipulation can also be achieved via acoustic radiation forces when the particle size is comparable to the TSAW wavelength. TSAWs applied perpendicular to the flow direction enable size-dependent separation within single-layer microchannels. Additionally, multilayer channel designs or internal microstructures can assist in localized separation or filtration. Since TSAW leakage waves propagate into the fluid at the Rayleigh angle, subsequent waves on the same side do not affect particles once they are displaced near the channel wall. This principle was utilized by Destgeer et al. (2015) to achieve the targeted separation of microparticles.

In addition, some methods can also be employed to modulate the traveling surface acoustic wave field to realize different forms of particle manipulation. By designing a three-way symmetric right-angle finger array, Wang et al. (2022) realized linear, clockwise and counterclockwise trajectory motions of suspended particles in a circular microchannel using ordered excitation of TSAW, as shown in Fig. 8(a). Devendran et al. (2017) found that the near-field diffraction of TSAW in the vicinity of the microchannel wall causes particles passing through the microfluid to displace, as shown in Fig. 8(b), which the team explained in detail using Fresnel's Huygens principle. In addition, by designing the wall structure of the microchannel to change the wavefront of the incident wave, it is possible to arrange the particles into various shapes by utilizing this diffraction effect (Collins et al., 2019; Raymond et al., 2020), as shown in Fig. 8(c), while the effective range of action is more limited.

Recently, Khan et al. (2024) developed an on-demand, label-free acoustic streaming fluid method based on the acoustic radiation force and torque induced by TSAW, which enables the separation of ellipsoids from spherical particles, as shown in Fig. 8(d). Liu et al. (2023b) developed a sorting system based on TSAW for the subsequent differential diagnosis of early dengue and tick-borne encephalitis, as shown in Fig. 8(e). Wang et al. (2024) used a TSAW technique based on a piezoelectric membrane acoustic wave platform to demonstrate that microparticles can be aligned, patterned and concentrated in circular and rectangular glass capillaries, as shown in Fig. 8(f).

The results show that the propagating SAWs can generate acoustic pressures and patterns in the fluid due to the diffractive effects, drag forces and acoustic radiation force, as functions of the resonant frequency and tilting angle of the SAW device. Geng et al. (2023) demonstrated an ultra-compact acoustic device for cell sorting, as shown in Fig. 8(g). This single actuator device allows for a non-invasive and label-free separation of living cells, thus providing greater flexibility and applicability. It employs narrow-path TSAW for precise separation of particle mixtures. Table 1 summarizes the literature on the SAW-based manipulation of particles and fluids demonstrated in subsection 4.

5. Conclusions and outlook

SAW microfluidic technology has advanced significantly in microfluidic and micro/nanoparticle manipulation, leveraging its advantages of non-contact nature, high precision and low energy consumption. This study provides a systematic and comprehensive review of microfluidics for surface acoustic wave on the basis of the theoretical framework of microfluidics

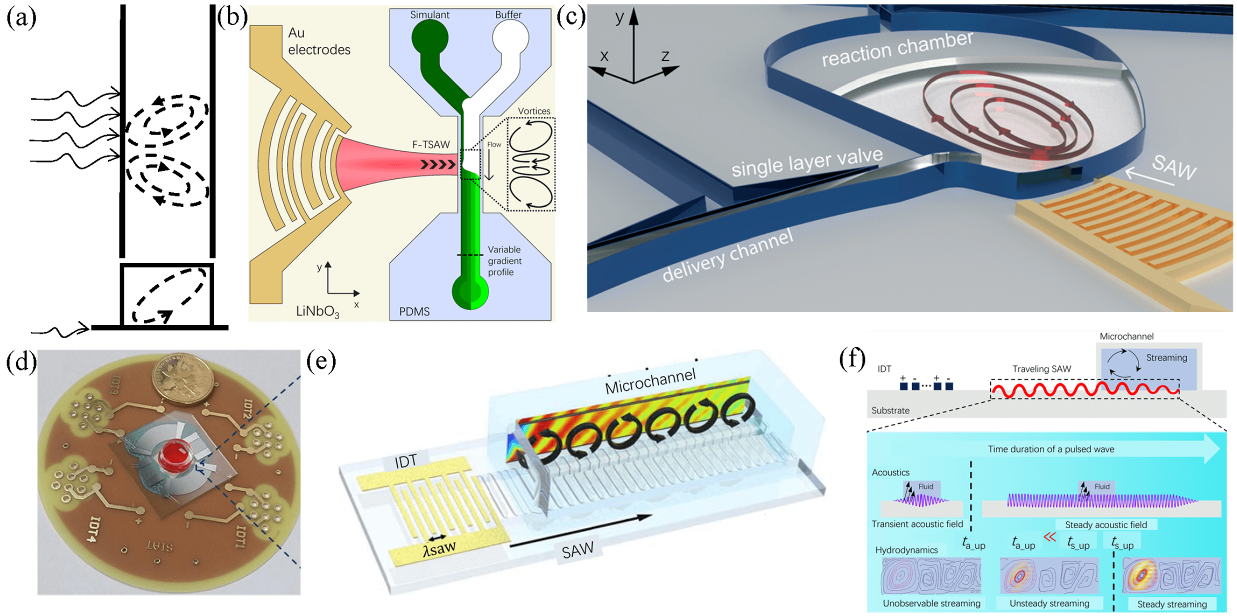

Fig. 7. Fluid mixing effects in microchannels under TSAW excitation. (a) Acoustic streaming fields in microchannels, (b) schematic diagram of the TSAW based gradient generator (Destgeer et al., 2014), (c) schematic of the reaction chamber (Zhang, et al., 2019), (d) optical imaging of high-intensity focused ultrasound device (Meng et al., 2015), (e) concept image showing vortices and acoustic radiation forces in a microchannel (Kolesnik et al., 2021) and (f) time scales of a SAW and large-scale streaming in a microchannel (Li et al., 2022).

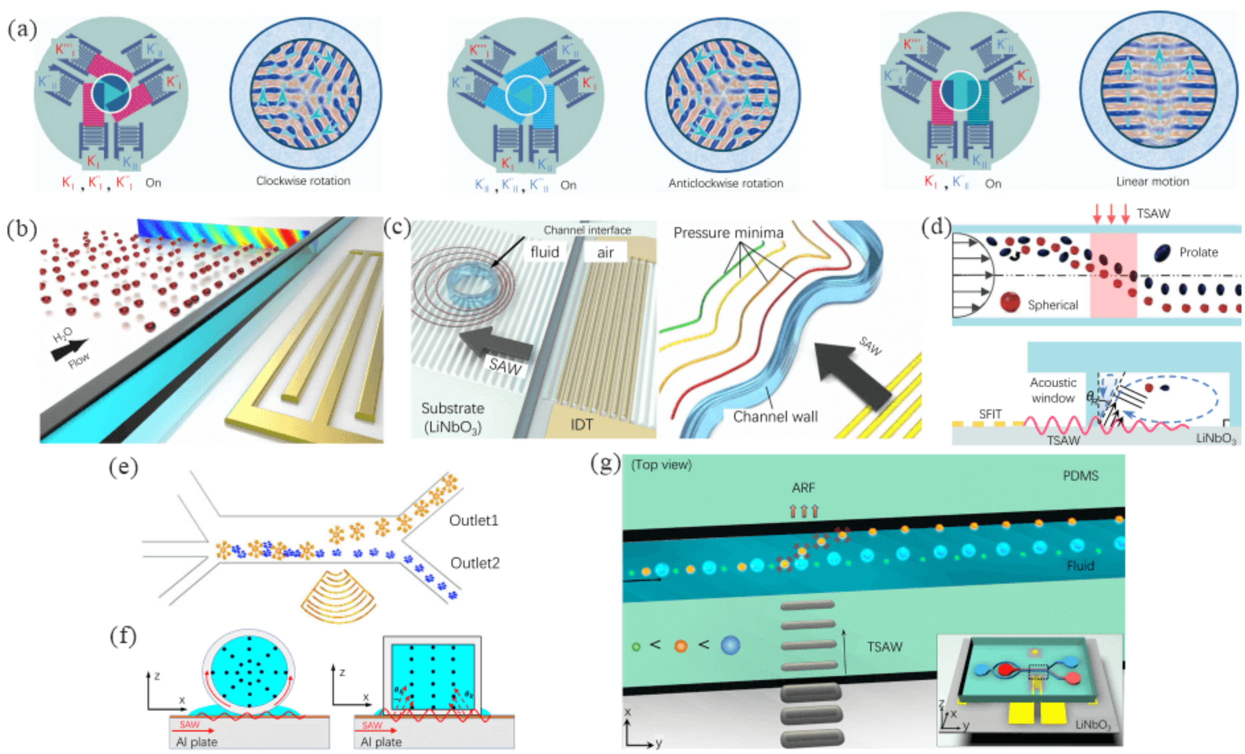

Fig. 8. Modulation of TSAW fields in microfluids. (a) Simulated acoustic pressure field patterns and trajectories (Wang et al., 2022), (b) drawing of a typical TSAW driven acoustofluidic systems (Devendran et al., 2017), (c) conceptual diagram of the interaction of an incident SAW with a channel interface (Collins et al., 2019; Raymond et al., 2020), (d) a channel of an acoustic streaming chip (Khan et al., 2024), (e) schematic of the process for sorting two different viruses (Liu et al., 2023a), (f) schematic of the acoustofluidic system (Wang et al., 2024) and (g) schematic diagram of the concept of a label-free cell sorting device (Geng et al., 2023).

Table 1. Summary of particle and fluid manipulation based on SAW.

Acoustic forms	Frequency (MHz)	Control object	Manipulation effects	References
SSAW	12.98	Particle (1-9.8 μm)	Separation of particles driven in two steps.	Chen et al. (2022)
SSAW	7.75	Platelet	High-purity platelet-poor plasma separated from whole blood without platelet activation.	Lim et al. (2025)
SSAW	12.8	Particle/platelet/cell (200 nm)	Special microchannels allow the otherwise competing acoustic streaming to complement the acoustic radiation effect.	Fakhfouri et al. (2023)
SSAW	9.4	Particle (2 μm)	Through morphologically reconfigurable magnetic microcolumn arrays, reconfigurable particle capture and droplet manipulation functions are achieved.	Pan et al. (2024)
TSAW	10	Particle/drop fluid	Allows acoustic streaming based on the density difference between the particles and the fluid to achieve separation.	Bourquin et al. (2014)
TSAW	15.3, 15.7, 20.3, 21.7	DNA segments/exosome subpopulations (< 100 nm)	Rapid (< 1 min) nanoparticle concentration and size-based separation	Gu et al. (2021)
TSAW	11-18	Particle (4-9 μm)	Ultrasonic isopycnic separation in sessile droplet/particle concentration	Qian et al. (2021)
TSAW	19.32	Polystyrene microparticles/ cancer cell (6/10/15 μm)	Patterning of cancer cells under an optimal contact angle condition	Nam et al. (2022)
TSAW	19.89, 33.15, 41.44	Polystyrene microparticles (500 nm)	Submicron particle enrichment within a spinning droplet	Peng et al. (2021)
TSAW	16.9	Diamond nanoparticles (100 nm)	Concentration of nanoparticles microcentrifugated in a sessile droplet	Akther et al. (2021)
TSAW	18.75	Microchannel fluid	Periodic, identically rotating Rayleigh streaming vortices	Kolesnik et al. (2021)
TSAW	24.6	Microchannel fluid	Slowly varying large-scale streaming in a microchannel	Li et al. (2022)
TSAW	10.8	Brine shrimp egg cells (30 μm)	Capture and steering of microparticles accurately according to pre-defined trajectories	Wang et al. (2022)
TSAW	141, 155	Polystyrene microparticles (5 μm)	Separation of prolate ellipsoids from spherical microparticles	Khan et al. (2024)
TSAW	50	Polystyrene microparticles (2/15 μm)	Employs polystyrene microspheres to capture virus and utilizes TSAW device to accomplish microsphere sorting according to particle size	Liu et al. (2023a)
TSAW	6.05	Polystyrene microparticles (3 μm)	Microparticles can be aligned, patterned and concentrated within both circular and rectangular glass capillaries	Wang et al. (2024)
TSAW	68.05	Polystyrene microparticles/blood cells/cancer cells (5/8/10/20 μm)	Isolation of 10 μm particles from mixture (5, 10, 20 μm) and separation of 8 and 10 μm particles	Geng et al. (2023)

and the principles of device design. The advantages and limitations of various IDT configurations are comprehensively discussed in the context of microfluidic application scenarios, including the impact of Brownian motion on the maneuvering efficiency and operational accuracy based on acoustic radiation forces, as well as acoustic streaming effects when the particle scale is too small. In addition, the advantages and disadvantages of IDT-based manipulation of particles and fluids in sessile droplets and microfluidic channels are evaluated, shedding light on the technological frontiers and challenges in this interdisciplinary field. By integrating the summaries and comparative evaluations, in order to establish the foundation for microfluidic technology studies based on SAW, the following future research directions are proposed:

1) In the context of standing wave systems, the prevailing acoustic standing waves primarily concentrate below 100 MHz frequencies (Novotny et al., 2022). To utilize standing wave effects for manipulating particles smaller than 100 nm, additional strategies are required, and higher frequencies and shorter wavelengths need to be investigated, such as the design of devices operating above GHz and improved acoustic field configurations. In addition, considerable research is underway to study secondary excitation structures that utilize auxiliary elements, in

order to extend the lower limit of particle manipulation.
2) To clarify the response of submicron and nanoscale particles under acoustic streaming, the nanoscale coupling of acoustic streaming and Brownian motion needs to be investigated, and the dynamics of particles below 100 nm needs to be modeled.
3) For biomedical applications, the SAW-induced flow control of nanoparticle self-assembly (2D arrays/chains) for novel optoelectronic devices and the real-time characterization of nanoparticles (size/density) can be implemented using high-frequency SAW for earlier and faster cancer cell or antibody detection. In addition, portable SAW chips can be used for rapid separation/detection of aqueous nano-contaminants (heavy metals/viruses) and for microbial screening of unlabeled foods.
4) In terms of manipulation accuracy, compared to optical and electrical methods, acoustic fluid manipulation is relatively limited in its ability to accurately control individual submicron to nanoscale particles. Thus, further in-depth studies are needed, especially for the manipulation and assisted detection of molecules such as nucleic acids, proteins, amino acids, and enzymes at the single-molecule level (Liu et al., 2022).
5) Acoustic streaming particle motion can be predicted using machine learning to adaptively optimize parameters (frequency/power). Deep learning can simulate complex fluid flows to guide IDT inverse design.

Acknowledgements

This work was supported by the National Natural Science Foundations of China (Nos. 11972132, 12272107 and 42172159).

Conflict of interest

The authors declare no competing interest.

References

Ai, Y., Sanders, C. K., Marrone, B. L. Separation of escherichia coli bacteria from peripheral blood mononuclear cells using standing surface acoustic waves. Analytical Chemistry, 2013, 85(19): 9126-9134.

Akthakul, A., Hochbaum, A. I., Stellacci, F., et al. Size fractionation of metal nanoparticles by membrane filtration. Advanced Materials, 2005, 17(5): 532-535.

Akther, A., Walsh, E. P., Reineck, P., et al. Acoustomicrofluidic concentration and signal enhancement of fluorescent nanodiamond sensors. Analytical Chemistry, 2021, 93(48): 16133-16141.

Ali, W. R., Prasad, M. Piezoelectric mems based acoustic sensors: A review. Sensors and Actuators A: Physical, 2020, 301: 111756.

Amorim, D., Sousa, P. C., Abreu, C., et al. A review of saw-based micro- and nanoparticle manipulation in microfluidics. Sensors, 2025, 25(5): 1577.

Astruc, D. Introduction: Nanoparticles in catalysis. Chemical Reviews, 2020, 120(2): 461-463.

Bausk, E., Taziev, R., Lee, A. Discrete apodization in quasi-slanted saw idts. In IEEE Symposium on Ultrasonics, 2003, 2: 1758-1761.

Bourquin, Y., Syed, A., Reboud, J., et al. Rare-Cell enrichment by a rapid, label-free, ultrasonic isopycnic technique for medical diagnostics. Angewandte Chemie International Edition, 2014, 53(22): 5587-5590.

Cai, J., Zhao, J., Zhong, J., et al. Microfluidic experiments and numerical simulation methods of pore-scale multiphase flow. Capillarity, 2024, 12(1): 1-5.

Chen, G., Gibson, K. J., Liu, D., et al. Regioselective surface encoding of nanoparticles for programmable self-assembly. Nature Materials, 2019, 18(2): 169-174.

Chen, X., Lv, H., Zhang, Y. A novel study on separation of particles driven in two steps based on standing surface acoustic waves. Chaos, Solitons & Fractals, 2022, 162: 112419.

Chen, Y., Nawaz, A. A., Zhao, Y., et al. Standing surface acoustic wave (ssaw)-based microfluidic cytometer. Lab on a Chip, 2014, 14(5): 916-923.

Choi, C., Choi, M. K., Hyeon, T., et al. Nanomaterial-Based soft electronics for healthcare applications. ChemNanoMat, 2016, 2(11): 1006-1017.

Collins, D. J., O'Rorke, R., Neild, A., et al. Acoustic fields and microfluidic patterning around embedded microstructures subject to surface acoustic waves. Soft Matter, 2019, 15(43): 8691-8705.

Deivasigamani, R., Mohd Maidin, N. N., Abdul Nasir, N. S., et al. A correlation of conductivity medium and bioparticle viability on dielectrophoresis-based biomedical applications. Electrophoresis, 2023, 44(5-6): 573-620.

Destgeer, G., Im, S., Ha, B. H., et al. Adjustable, rapidly switching microfluidic gradient generation using focused travelling surface acoustic waves. Applied Physics Letters, 2014, 104(2): 023506.

Destgeer, G., Ha, B. H., Park, J., et al. Microchannel anechoic corner for microparticle manipulation via travelling surface acoustic waves. Physics Procedia, 2015, 70: 30-33.

Destgeer, G., Jung, J. H., Park, J., et al. Particle separation inside a sessile droplet with variable contact angle using surface acoustic waves. Analytical Chemistry, 2017, 89(1): 736-744.

Devendran, C., Collins, D. J., Ai, Y., et al. Huygens-fresnel acoustic interference and the development of robust time-averaged patterns from traveling surface acoustic waves. Physical Review Letters, 2017, 118(15): 154501.

Ding, X., Lin, S. C. S., Kiraly, B., et al. On-chip manipulation of single microparticles, cells, and organisms using surface acoustic waves. Proceedings of the National Academy of Sciences of the United States of America, 2012a, 109(28): 11105-11109.

Ding, X., Peng, Z., Lin, S. C. S., et al. Cell separation using tilted-angle standing surface acoustic waves. Proceedings of the National Academy of Sciences of the United States of America, 2014, 111(36): 12992-12997.

Ding, X., Shi, J., Lin, S. C. S., et al. Tunable patterning of microparticles and cells using standing surface acoustic waves. Lab on a Chip, 2012b, 12(14): 2491-2497.

Doinikov, A. A., Thibault, P., Marmottant, P. Acoustic streaming induced by two orthogonal ultrasound standing waves in a microfluidic channel. Ultrasonics, 2018, 87: 7-19.

Dürr, M., Kentsch, J., Müller, T., et al. Microdevices for manipulation and accumulation of micro- and nanoparticles by dielectrophoresis. Electrophoresis, 2003, 24(4): 722-731.

Fakhfouri, A., Colditz, M., Devendran, C., et al. Fully microfabricated surface acoustic wave tweezer for collection of submicron particles and human blood cells. ACS Applied Materials & Interfaces, 2023, 15(20): 24023-24033.

Falkovich, G. Fluid Mechanics: A Short Course for Physicists. New York, USA, Cambridge University Press, 2011.

Fan, Y., Wang, X., Ren, J., et al. Recent advances in acoustofluidic separation technology in biology. Microsystems & Nanoengineering, 2022, 8(1): 94.

Friend, J., Yeo, L. Y. Microscale acoustofluidics: Microfluidics driven via acoustics and ultrasonics. Reviews of Modern Physics, 2011, 83(2): 647-704.

Geng, W., Liu, Y., Yu, N., et al. An ultra-compact acoustofluidic device based on the narrow-path travelling surface acoustic wave (np-tsaw) for label-free isolation of living circulating tumor cells. Analytica Chimica Acta, 2023, 1255: 341138.

Gu, Y., Chen, C., Mao, Z., et al. Acoustofluidic centrifuge for nanoparticle enrichment and separation. Science Advances, 2021, 7(1): eabc0467.

Hossein, F., Angeli, P. A review of acoustofluidic separation of bioparticles. Biophysical Reviews, 2023, 15(6): 2005-2025.

Hsu, J. C. Enhanced micromixing using surface acoustic wave devices: Fundamentals, designs, and applications. Micromachines, 2025, 16(6): 619.

Huang, J., Kim, F., Tao, A. R., et al. Spontaneous formation of nanoparticle stripe patterns through dewetting. Nature Materials, 2005, 4(12): 896-900.

Jang, J., Lee, S. S. Theoretical and experimental study of mhd (magnetohydrodynamic) micropump. Sensors and Actuators A: Physical, 2000, 80(1): 84-89.

Jo, M., Seo, Y. W., Yoon, H., et al. Embedded metallic nanoparticles facilitate metastability of switchable metallic domains in mott threshold switches. Nature Communications, 2022, 13(1): 4609.

Kaushik, M. Sound wave propagation in compressible fluids and flow regimes, in Fundamentals of Gas Dynamics, edited by Kaushik, M, Springer Singapore, Singapore, pp. 109-136, 2022.

Khan, M. S., Ali, M., Lee, S. H., et al. Acoustofluidic separation of prolate and spherical micro-objects. Microsystems & Nanoengineering, 2024, 10(1): 6.

Kolesnik, K., Hashemzadeh, P., Peng, D., et al. Periodic rayleigh streaming vortices and eckart flow arising from traveling-wave-based diffractive acoustic fields. Physical Review E, 2021, 104(4): 045104.

Kondoh, J., Okiyama, Y., Mikuni, S., et al. Development of a shear horizontal surface acoustic wave sensor system for liquids with a floating electrode unidirectional transducer. Japanese Journal of Applied Physics, 2008, 47(5S): 4065.

Kondoh, J., Shimizu, N., Matsui, Y., et al. Development of temperature-control system for liquid droplet using surface acoustic wave devices. Sensors and Actuators A: Physical, 2009, 149(2): 292-297.

Koo, K., Shen, B., Baik, S. I., et al. Formation mechanism of high-index faceted pt-bi alloy nanoparticles by evaporation-induced growth from metal salts. Nature Communications, 2023, 14(1): 3790.

Kuljabekov, A., Ashirbekov, A., Wang, L., et al. Isothermal co2 injection into water-saturated porous media: Lattice-boltzmann modelling of pulsatile flow with porosity, tortuosity, and optimal frequency characterization. Thermal Science and Engineering Progress, 2023, 43: 101949.

Lee, S. H., Cha, B., Yi, H., et al. Acoustofluidic separation of bacteria from platelets using tilted-angle standing surface acoustic wave. Sensors and Actuators B: Chemical, 2024, 417: 136161.

Lee, C. S., Lee, H., Westervelt, R. M. Microelectromagnets for the control of magnetic nanoparticles. Applied Physics Letters, 2001, 79(20): 3308-3310.

Li, J., Esteban-Fernández De Ávila, B., Gao, W., et al. Micro/nanorobots for biomedicine: Delivery, surgery, sensing, and detoxification. Science Robotics, 2017, 2(4): eaam6431.

Li, L., Jia, K., Yang, K. Unsteady time-averaged streaming in microfluidics using traveling surface acoustic waves. Microfluidics and Nanofluidics, 2022, 26(10): 75.

Li, M., Lohmüller, T., Feldmann, J. Optical injection of gold nanoparticles into living cells. Nano Letters, 2015, 15(1): 770-775.

Li, W., Yao, Z., Ma, T., et al. Acoustofluidic precise manipulation: Recent advances in applications for micro/nano bioparticles. Advances in Colloid and Interface Science, 2024, 332: 103276.

Lighthill, S. J. Acoustic streaming. Journal of Sound and Vibration, 1978, 61(3): 391-418.

Lim, H., Hong, S., Cho, S., et al. Advanced design of indented-standing surface acoustic wave (i-ssaw) device for platelet-derived microparticle separation from whole blood. Sensors and Actuators B: Chemical, 2025, 423: 136742.

Liu, X., Chen, X., Dong, Y., et al. Multiple virus sorting based on aptamer-modified microspheres in a tsaw device. Microsystems & Nanoengineering, 2023a, 9(1): 64.

Liu, X., Chen, X., Yang, Z., et al. Surface acoustic wave based microfluidic devices for biological applications. Sensors & Diagnostics, 2023b, 2(3): 507-528.

Liu, W., Gao, H., Liu, K., et al. A review on particle assembly in standing wave acoustic field. Journal of Nanoparticle Research, 2022, 24(4): 81.

Liu, R. H., Yang, J., Pindera, M. Z., et al. Bubble-induced acoustic micromixing. Lab on a Chip, 2002, 2(3): 151-157.

Lomeli-Martin, A., Ahamed, N., Abhyankar, V. V., et al. Electropatterning-contemporary developments for selective particle arrangements employing electrokinetics. Electrophoresis, 2023, 44(11-12): 884-909.

Meng, L., Deng, Z., Niu, L., et al. A disposable microfluidic device for controlled drug release from thermal-sensitive liposomes by high intensity focused ultrasound. Theranostics, 2015, 5(11): 1203-1213.

Mitragotri, S., Anderson, D. G., Chen, X., et al. Accelerating the translation of nanomaterials in biomedicine. ACS Nano, 2015, 9(7): 6644-6654.

Mullard, A. FDA approves 100th monoclonal antibody product. Nature Reviews Drug Discovery, 2021, 20(7): 491-495.

Nakagomi, S., Asano, H., Tanaka, H., et al. Single-phase unidirectional surface acoustic wave transducer using cu electrode. Japanese Journal of Applied Physics, 2003, 42(5B): 3152-3156.

Nam, H., Sung, H. J., Park, J., et al. Manipulation of cancer cells in a sessile droplet via travelling surface acoustic waves. Lab on a Chip, 2022, 22(1): 47-56.

Novotny, J., Lenshof, A., Laurell, T. Acoustofluidic platforms for particle manipulation. Electrophoresis, 2022, 43(7-8): 804-818.

Nyborg, W. L. Acoustic streaming, in Nonlinear Acoustics, edited by Hamilton M and Blackstock D, Springer Nature, Switzerland, Cham, pp. 205-229, 2024.

Orosco, J., Friend, J. Modeling fast acoustic streaming: Steady-state and transient flow solutions. Physical Review E, 2022, 106(4): 045101.

Pan, H., Mei, D., Han, S., et al. Morphologically reconfigurable magnetic micropillar arrays using acoustic streaming for particle capture and droplet manipulation. Sensors and Actuators B: Chemical, 2024, 412: 135776.

Park, J., Ha, B. H., Destgeer, G., et al. An acoustothermal heater for paper microfluidics towards point-of-care glucose detection. Physics Procedia, 2015, 70: 46-49.

Peng, T., Fan, C., Zhou, M., et al. Rapid enrichment of submicron particles within a spinning droplet driven by a unidirectional acoustic transducer. Analytical Chemistry, 2021, 93(39): 13293-13301.

Peng, T., Lin, X., Li, L., et al. Investigation on submicron particle separation and deflection using tilted-angle standing surface acoustic wave microfluidics. Heliyon, 2024, 10(3): e25042.

Potter, G., Tokranova, N., Rastegar, A., et al. Design, fabrication, and testing of surface acoustic wave devices for semiconductor cleaning applications. Microelectronic Engineering, 2016, 162: 100-104.

Poudineh, M., Aldridge, P. M., Ahmed, S., et al. Tracking the dynamics of circulating tumour cell phenotypes using nanoparticle-mediated magnetic ranking. Nature Nanotechnology, 2017, 12(3): 274-281.

Qi, A., Yeo, L. Y., Friend, J. R. Interfacial destabilization and atomization driven by surface acoustic waves. Physics of Fluids, 2008, 20(7): 074103.

Qi, M., Dang, D., Yang, X., et al. Surface acoustic wave manipulation of bioparticles. Soft Matter, 2023, 19(23): 4166-4187.

Qian, J., Begum, H., Song, Y., et al. Plug-and-play acoustic tweezer enables droplet centrifugation on silicon superstrate with surface multi-layered microstructures. Sensors and Actuators A: Physical, 2021, 321: 112432.

Raghavan, R. V., Friend, J. R., Yeo, L. Y. Particle concentration via acoustically driven microcentrifugation: Micropiv flow visualization and numerical modelling studies. Microfluidics and Nanofluidics, 2010, 8(1): 73-84.

Rajapaksa, A., Qi, A., Yeo, L. Y., et al. Enabling practical surface acoustic wave nebulizer drug delivery via amplitude modulation. Lab on a Chip, 2014, 14(11): 1858-1865.

Ramezani, H., Dietz, H. Building machines with dna molecules. Nature Reviews Genetics, 2020, 21(1): 5-26.

Raymond, S. J., Collins, D. J., O'Rorke, R., et al. A deep learning approach for designed diffraction-based acoustic patterning in microchannels. Scientific Reports, 2020, 10(1): 8745.

Renaudin, A., Tabourier, P., Zhang, V., et al. SAW nanopump for handling droplets in view of biological applications. Sensors and Actuators B: Chemical, 2006, 113(1): 389-397.

Roux-Marchand, T., Beyssen, D., Sarry, F., et al. Rayleigh surface acoustic wave as an efficient heating system for biological reactions: Investigation of microdroplet temperature uniformity. IEEE Transactions on Ultrasonics, Ferroelectrics, and Frequency Control, 2015, 62(4): 729-735.

Sesen, M., Alan, T., Neild, A. Microfluidic on-demand droplet merging using surface acoustic waves. Lab on a Chip, 2014, 14(17): 3325-3333.

Shilton, R. J., Mattoli, V., Travagliati, M., et al. Rapid and controllable digital microfluidic heating by surface acoustic waves. Advanced Functional Materials, 2015, 25(37): 5895-5901.

Shilton, R. J., Travagliati, M., Beltram, F., et al. Nanoliter-Droplet acoustic streaming via ultra high frequency surface acoustic waves. Advanced Materials, 2014, 26(29): 4941-4946.

Song, Y., Li, D., Xuan, X. Recent advances in multimode microfluidic separation of particles and cells. Electrophoresis, 2023, 44(11-12): 910-937.

Sritharan, K., Strobl, C. J., Schneider, M. F., et al. Acoustic mixing at low reynold's numbers. Applied Physics Letters, 2006, 88(5): 054102.

Sun, J., Xianyu, Y., Jiang, X. Point-of-care biochemical assays using gold nanoparticle-implemented microfluidics. Chemical Society Reviews, 2014, 43(17): 6239-6953.

Tan, M. K., Friend, J. R., Yeo, L. Y. Microparticle collection and concentration via a miniature surface acoustic wave device. Lab on a Chip, 2007, 7(5): 618-625.

Tiller, B., Reboud, J., Tassieri, M., et al. Frequency dependence of microflows upon acoustic interactions with fluids. Physics of Fluids, 2017, 29(12): 122008.

Vuong, T., Qi, A., Muradoglu, M., et al. Precise drop dispensation on superhydrophobic surfaces using acoustic nebulization. Soft Matter, 2013, 9(13): 3631.

Wang, W., Chen, Y., Farooq, U., et al. Ultrafast chemical-free cell lysis by high speed stream collision induced by surface acoustic waves. Applied Physics Letters, 2017, 110(14): 143504.

Wang, Q., Maramizonouz, S., Martin, M. S., et al. Acoustofluidic patterning in glass capillaries using travelling acoustic waves based on thin film flexible platform. Ultrasonics, 2024, 136: 107149.

Wang, Y., Pan, H., Mei, D., et al. Programmable motion control and trajectory manipulation of microparticles through tri-directional symmetrical acoustic tweezers. Lab on a Chip, 2022, 22(6): 1149-1161.

Wang, L., Parsa, E., Gao, Y., et al. Experimental study and modeling of the effect of nanoconfinement on hydrocarbon phase behavior in unconventional reservoirs. Paper SPE 169581 Presented at the SPE Western North American and Rocky Mountain Joint Meeting, Denver, Colorado, 17-18 April, 2014.

Wei, W., Wang, Z., Wang, B., et al. Acoustofluidic manipulation for submicron to nanoparticles. Electrophoresis, 2024, 45(23-24): 2132-2153.

White, R. M., Voltmer, F. W. Direct piezoelectric coupling to surface elastic waves. Applied Physics Letters, 1965, 7(12): 314-316.

Wiklund, M., Green, R., Ohlin, M. Acoustofluidics 14: Applications of acoustic streaming in microfluidic devices. Lab on a Chip, 2012, 12(14): 2438-2451.

Wixforth, A., Strobl, C., Gauer, C., et al. Acoustic manipulation of small droplets. Analytical and Bioanalytical Chemistry, 2004, 379(7-8): 982-991.

Wu, M. C. Optoelectronic tweezers. Nature Photonics, 2011, 5(6): 322-324.

Wu, R., Liu, X., and Gong, X. A study of the acoustical radiation force considering attenuation. Science China Physics, Mechanics & Astronomy, 2013, 56(7): 1237-1245.

Wu, M., Ouyang, Y., Wang, Z., et al. Isolation of exosomes from whole blood by integrating acoustics and microfluidics. Proceedings of the National Academy of Sciences of the United States of America, 2017, 114(40): 10584-10589.

Xia, Q., Chen, Z., Xiao, P., et al. Fermi level-tuned optics of graphene for attocoulomb-scale quantification of electron transfer at single gold nanoparticles. Nature Communications, 2019, 10(1): 3849.

Xu, L., Wang, X., Liu, Y., et al. Lipid nanoparticles for drug delivery. Advanced NanoBiomed Research, 2022, 2(2): 2100109.

Yang, S., Tian, Z., Wang, Z., et al. Harmonic acoustics for dynamic and selective particle manipulation. Nature Materials, 2022a, 21(5): 540-546.

Yang, Y., Zhang, L., Jin, K., et al. Self-adaptive virtual microchannel for continuous enrichment and separation of nanoparticles. Science Advances, 2022b, 8(30): eabn8440.

Shui, Y., Lin, J., Wu, H., et al. Optimization of single-phase, unidirectional transducers using three fingers per period. IEEE Transactions on Ultrasonics, Ferroelectrics and Frequency Control, 2002, 49(12): 1617-1621.

Zhang, P., Bachman, H., Ozcelik, A., et al. Acoustic microfluidics. Annual Review of Analytical Chemistry, 2020a, 13(1): 17-43.

Zhang, Y., Chen, X. Particle separation in microfluidics using different modal ultrasonic standing waves. Ultrasonics Sonochemistry, 2021, 75: 105603.

Zhang, S., Chen, C., Xue, C., et al. Ribbon of dna lattice on gold nanoparticles for selective drug delivery to cancer cells. Angewandte Chemie International Edition, 2020b, 59(34): 14584-14592.

Zhang, Y., Devendran, C., Lupton, C., et al. Versatile platform for performing protocols on a chip utilizing surface acoustic wave (saw) driven mixing. Lab on a Chip, 2019, 19(2): 262-271.

Zhang, P., Rufo, J., Chen, C., et al. Acoustoelectronic nanotweezers enable dynamic and large-scale control of nanomaterials. Nature Communications, 2021, 12(1): 3844.

Zhao, L, Niu, P., Casals, E., et al. Phase separation of a nonionic surfactant aqueous solution in a standing surface acoustic wave for submicron particle manipulation. Lab on a Chip, 2021a, 21(4): 660-667.

Zhao, L, Takimoto, T., Ito, M., et al. Chromatographic separation of highly soluble diamond nanoparticles prepared by polyglycerol grafting. Angewandte Chemie International Edition, 2011, 50(6): 1388-1392.

Zhao, X., Yang, L., Guo, J., et al. Transistors and logic circuits based on metal nanoparticles and ionic gradients. Nature Electronics, 2021b, 4(2): 109-115.

Zheng, T., Wang, C., Hu, Q., et al. The role of electric field in microfluidic heating induced by standing surface acoustic waves. Applied Physics Letters, 2018, 112(23): 233702.

Zhou, Y., Guan, W., Zhao, C., et al. Spontaneous imbibition behavior in porous media with various hydraulic fracture propagations: A pore-scale perspective. Advance in Geo-Energy Research, 2023, 9(3): 185-197.

Zhou, Y., Guan, W., Zhao, C., et al. Numerical methods to simulate spontaneous imbibition in microscopic pore structures: A review. Capillarity, 2024, 11(1): 1-21.

Zhou, L., Shi, Y., Zhu, X., et al. Recent progress on optical micro/nanomanipulations: Structured forces, structured particles, and synergetic applications. ACS Nano, 2022, 16(9): 13264-13278.

Zhou, J., Tao, X., Luo, J., et al. Nebulization using zno/si surface acoustic wave devices with focused interdigitated transducers. Surface and Coatings Technology, 2019, 367: 127-134.